

# Damage Identification of Nonlinear Structural Systems

Lai-Ah Wong\* and Jay-Chung Chen†

*Hong Kong University of Science and Technology, Clear Water Bay, Kowloon, Hong Kong,  
People's Republic of China*

The present investigation develops methods for the identification of highly localized structural damages in nonlinear structures. The damage is defined as either a reduction of stiffness or a change of restoring force characteristics from linear (undamaged state) to weak nonlinear (damaged state). One method for identifying both the location and type of damages is the location vector method (LVM). The other method is for quantifying the damage. The LVM requires only the modal data from the first few fundamental modes. The second method is based on fast Fourier transform (FFT) and the least-squares method under the assumptions that the location of the damages can be identified and their responses can be measured by testing. Without loss of generality, the methods are illustrated by a five-degree-of-freedom Duffing's nonlinear system. Measurement data are simulated in the time domain and in the frequency domain by using the Runge-Kutta method and FFT, respectively. The robustness and effectiveness of the methods are examined by using a simulated output time history contaminated by a 5% white noise, which represents more realistic levels of measurement errors.

## Nomenclature

$A$	= unknown identification parameters vector
$a_{1s}, a_{1s}$	= unknown identification parameters
$B$	= influence coefficients matrix of the input forcing function
$C$	= influence coefficients matrix of the output displacement vector
$K_{eq}$	= equivalent linear stiffness matrix in the damage state of the structure
$K_o$	= stiffness matrix in the original state of the structure
$L(Y)$	= location vector
$M_o$	= mass matrix in the original state of the structure
$P_o$	= damping matrix in the original state of the structure
$U$	= amplitude vector of the input harmonic excitation
$u(t), y(t)$	= input harmonic excitation forcing function and output displacement response vector
$X_j(Y)$	= mode shape vector of the damaged structure
$x(t), \dot{x}(t), \ddot{x}(t)$	= displacement, velocity, and acceleration response vector
$\Gamma$	= nonlinear stiffness matrix
$\Delta$	= variation sign
$\Phi$	= identification coefficients matrix
$\Psi$	= influence coefficient matrix of linear and nonlinear terms of the restoring forces of the damaged joints
$\psi$	= nonlinear operator
$\Omega$	= harmonic excitation frequency
$\omega$	= natural frequency

## Introduction

IT is important that structural integrity or structural health information are available or can be estimated at all times for determining the reliability and safety of nonlinear structural systems. However, the structural damages that affect the integrity and safety

may not be obvious and are difficult to estimate by inspection. One approach to assess the damages is by using the structural-system identification techniques.

Structural system identification within the linear region has been well developed. Many techniques have been proposed with varying degrees of success.<sup>1-4</sup> These methodologies have also been applied to structural damage assessment in which structural element stiffness reduction can be identified by examining their response behaviors. However, the question of whether a structure is still linear after the damage remains. This is very important because the dynamical behaviors of a nonlinear system can be quite different from those of its associated linear system. If the restoring characteristic of the local elements is changed from linear to Duffing's nonlinear (softening) because of material yielding in the structure, the structure may change into an unstable state, and much larger damage can occur when an external loading reaches a critical value. Also if the structural system becomes nonlinear after damage, its dynamical characteristics cannot be estimated by using linear system identification methods. In the mean time the identification for damage can be more significant for the case of a weak nonlinear structure than that of a strong nonlinear structure. The next question is whether linear identification techniques can be generalized for the weak nonlinear structural systems at the initial state of damage.

The present study is an attempt at identifying the location, type, and size of local damage in the weak nonlinear structures. The assumption is made that 1) a structure is linear in undamaged state and 2) the damage is defined either as a reduction of stiffness or a change in restoring characteristic of the structures from linear to weak nonlinear. Two methods have been developed: one is the location vector method (LVM) to identify the location of local damaged elements in the structures, and the other is to identify the type and size of the damage.

The LVM is developed for defining a location vector based on the variation form of the equivalent linearization characteristic equation of a weak nonlinear structure. The natural frequency and mode shape defined in this characteristic equation are the functions of the structural parameters such as the inertia and stiffness properties. The degree of nonlinearity in the structure is defined in such a way that the linear characteristic will be realized when the nonlinearity diminishes. This means that the eigenparameters (natural frequency and normal mode) will change if the local structural parameters change before and after the damage. Recognizing the eigenparameters will be changing because of nonlinearities in the local elements, the nonlinearity will be assumed to be very small, and the linear identification method can be applied. The main advantage of LVM is that it only needs to be measuring data of eigenparameters for the first few fundamental modes. This is an important aspect because

Received 18 December 1998; revision received 17 September 1999; accepted for publication 13 December 1999. Copyright © 2000 by the American Institute of Aeronautics and Astronautics, Inc. All rights reserved.

\*Assistant Research Engineer, Center for Coastal and Atmospheric Research; wla@ust.hk.

†Professor, Department of Mechanical Engineering, and Acting Director of Center for Coastal and Atmospheric Research; jccchen@ust.hk. Member AIAA.

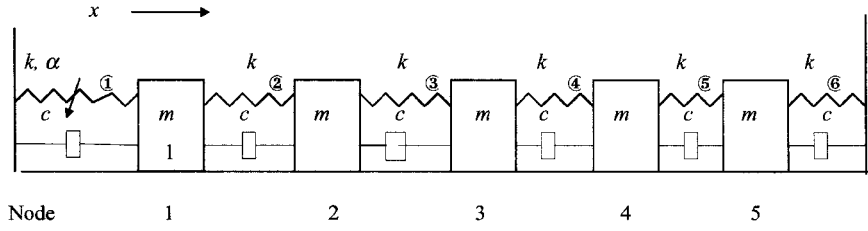


Fig. 1 Five-degree-of-freedom structural system.

only the first few natural frequencies and modes can be measured for most real situation cases.<sup>5</sup>

The errors of LVM depend on both the measuring errors of the lowest eigenparameters and the degree of the damage in the structure. In general, LVM is applicable when the relative measurement error  $\varepsilon$  of the lowest natural frequency  $\omega$  is less than one order of the relative change ( $\gamma = \Delta\omega/\omega$ ) of the frequency before and after the damage. For example, if  $\gamma$  is  $\mathcal{O}(10^{-1})$ ,  $\varepsilon$  should be at least  $\mathcal{O}(10^{-2})$ . In general, the value of  $\varepsilon$  is about 10% (Ref. 5) so that  $\gamma$  must be larger than 10%. This means that the damage detection process can be initiated when the changes of natural frequency are not small.

Quantifying the size of damage is also an inverse problem such that it depends on available input/output data of the structural systems. The more input/output data are available, the easier is the identification. However, for most of the real structures, not all output data are available, which makes the identification of the size of damage more difficult and complicated. But, after identification of the location of damage is solved, the quantifying problem can be simplified by directly measuring the responses of the damaged elements for a given input excitation. From the view of this simplification, an estimation of the type and size of the damage is developed based on the relationship of structural input/output data in the frequency domain. The identification model is established by using fast Fourier transform (FFT),<sup>6</sup> and the identification algorithm is established by using the least-squares method (LSM).<sup>7</sup>

Without the loss of generality, the methods are illustrated by analyzing a five-degree-of-freedom spring/mass Duffing's nonlinear system as shown in Fig. 1. Measurement is simulated in the time domain and frequency domain by using the Runge-Kutta method<sup>8</sup> and FFT, respectively. The robustness and effectiveness of the methods are examined by using simulated output time history contaminated by white noise with strength about 5–10% (in respect to the amplitude of response), which represents more realistic levels of model and measurement errors.

### Equivalent Natural Frequency and Mode Shape Vector

The assumption is made that of an  $n$ -degree-of-freedom structural system is linear before the damage, and its governing differential equation is represented as

$$M_o \ddot{x}(t) + P_o \dot{x}(t) + K_o x = Bu(t) \quad (1)$$

where  $x$  is a physical displacement vector and  $u$  is a  $m \times 1$  vector of harmonic excitation forces.

After the damage, it changes into

$$M_o \ddot{x}(t) + P_o \dot{x}(t) + K_o x(t) + \Delta K_L x(t) + \Gamma \psi[y(t)] = Bu(t) \quad (2)$$

$$y(t) = Cx(t)$$

where  $\Delta K_L$  is an  $n \times n$  negative and symmetry matrix that denotes the reduction of linear stiffness of the structural system before and after the change. One can say that  $\Delta K_L$  is independent of the responses of the system according to linear dynamics theory and  $y$  is a relative displacement vector of the nonlinear elements.

The undamped and homogeneous equation (2) can be written as

$$M_o \ddot{x}(t) + K_o x(t) + \Delta K_L x(t) + \Gamma \psi[y(t)] = 0 \quad (3)$$

$$y(t) = Cx(t)$$

For Eq. (3) one can write a particular solution in explicit form:

$$x(t) = X e^{i\omega t}, \quad y(t) = Y e^{i\omega t} \quad (4)$$

where  $X$  is the amplitude of the displacement vector and  $Y$  is the amplitude of the relative displacement vector of nonlinear elements;  $\omega$  is the frequency of the periodic in solution.

The assumption is made that the nonlinear function vector in Eq. (3) can be expanded into a Fourier series, i.e.,

$$\psi[y(t)] = \psi(Y e^{i\omega t}) = \Psi(Y) e^{i\omega t} + \dots = \eta(Y) Y e^{i\omega t} + \dots \quad (5)$$

where  $\Psi(Y)$  is the first-term Fourier coefficient vector and  $\Psi(Y) = \eta(Y) Y$ .

By substituting Eqs. (4) and (5) into Eq. (3), one obtains

$$[K_o + \Delta K_L + \Delta K_{NL}(Y) - \omega^2 M_o] X = 0 \quad (6a)$$

where  $\Delta K_{NL}(Y) = \Gamma \eta(Y) C$  is defined as an  $n \times n$  negative and symmetry matrix so that its physical significance is an equivalent linearization stiffness matrix of nonlinear term in Eq. (3). It is dependent on the amplitudes of responses of the nonlinear elements. Equation (6a) can be rewritten as

$$[K_{eq}(Y) - \omega^2(Y) M_o] X(Y) = 0 \quad (6b)$$

where  $K_{eq}(Y) = K_o + \Delta K_L + \Delta K_{NL}(Y) = K_o + \Delta K$  is called the equivalent linearization stiffness matrix of the nonlinear structures; and  $\Delta K$  is the negative (or zero) variation matrix of the stiffness before and after the change.  $\Delta K = 0$  means that no stiffness damage appears in the structure, i.e.,  $\lim_{\Delta K \rightarrow 0} K_{eq} = K_o$ .

Similar to a linear eigenvalue problem definition, here Eq. (6b) can be defined as the equivalent linearization eigenvalue equation of the weak nonlinear structural systems. When the nonlinearity of the structures is vanished, i.e.,  $\Delta K_{NL}$  is equal to zero, Eq. (6b) will become an eigenvalue equation of the linear structural systems. Equation (6b) is a homogeneous algebra equation with  $n$  pairs of the eigensolutions that are called the eigenvalues and eigenvectors. Let  $\lambda_j(Y)$  and  $\phi_j(Y)$  denote the  $j$ th eigenvalue and eigenvector of Eq. (6b); respectively, one has

$$\lambda_j(Y) = \omega_j^2(Y), \quad \phi_j(Y) = X_j(Y), \quad j = 1, 2, \dots, n \quad (7)$$

where  $\omega_j(Y)$  and  $X_j(Y)$  are defined as the  $j$ th equivalent natural frequency and mode shape vector of the weak nonlinear system, respectively. According to the nonlinear dynamical theory,<sup>9–11</sup> the main characteristics of equivalent natural frequency and natural mode are that 1) they are functions of the amplitude of responses of the nonlinear elements and the linear characteristics can be realized when the nonlinearity diminishes, as shown in Fig. 2, i.e.,

$$\lim_{\Gamma \rightarrow 0, \text{ or } Y \rightarrow 0} [\omega_j(Y)] = \omega_j^{(L)}, \quad \lim_{\Gamma \rightarrow 0, \text{ or } Y \rightarrow 0} [X_j(Y)] = X_j^{(L)} \quad (8)$$

$$j = 1, 2, 3, \dots, n$$

where  $\omega_j^{(L)}$  and  $X_j^{(L)}$  denote the  $j$ th-order natural frequency and the mode shape vector of the associated linear systems; 2) the resonance will occur, as the external harmonic excitation frequency approaches one of the equivalent natural frequencies, and the resonance peaks of response in the frequency domain will appear at the equivalent natural frequencies such that the equivalent natural frequencies and mode shape vectors can be determined by the locations and magnitudes of these peaks as shown in Fig. 3; 3) the magnitudes of the components in the equivalent mode vector are not unique, but the ratio values between each other are unique; 4) the equivalent natural frequencies and modes will satisfy the equation

$$\lim_{\Delta K \rightarrow 0} \omega_j(Y) = \omega_{oj}, \quad \lim_{\Delta K \rightarrow 0} X_j(Y) = X_{oj} \quad (9)$$

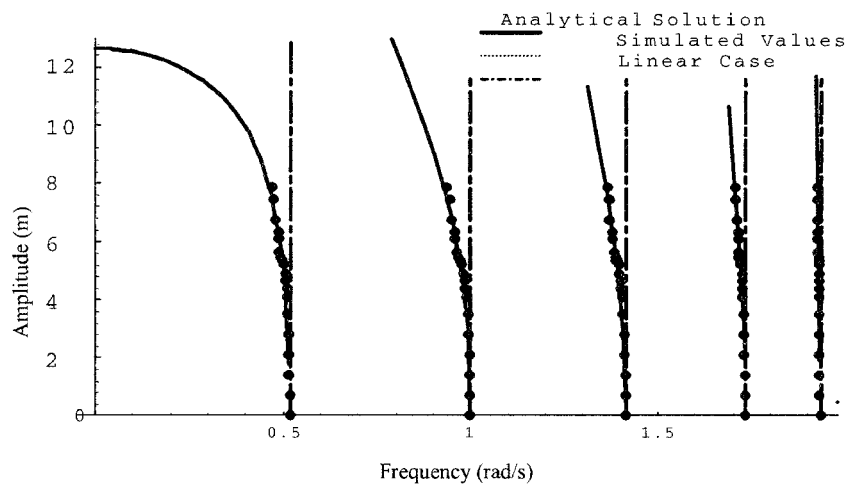


Fig. 2 Relationships of output amplitude vs equivalent natural frequencies.

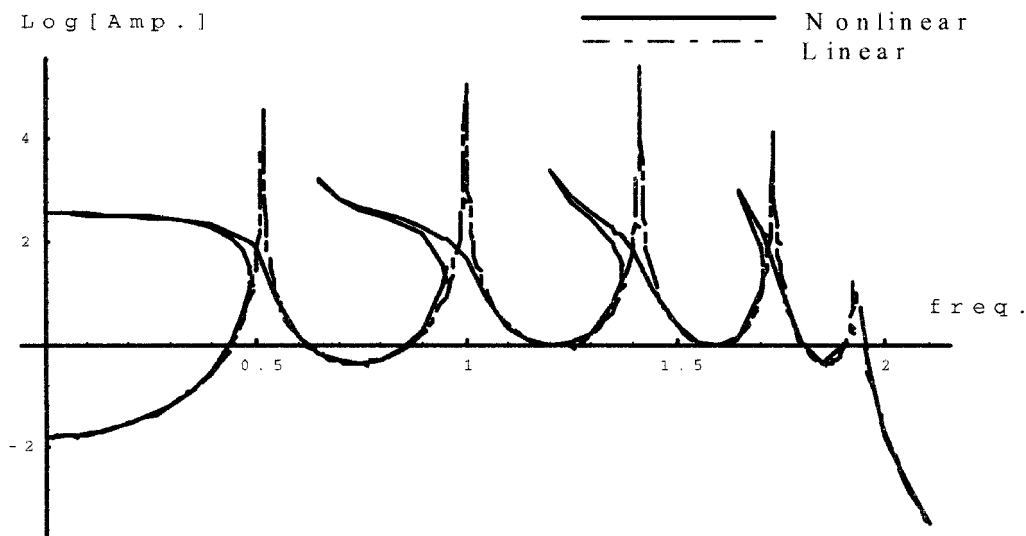


Fig. 3 Relationship of the output amplitude vs excitation frequency.

where  $\omega_{oj}$  and  $X_{oj}$  denote the  $j$ th-order original designing natural frequency and the mode shape vector of the structure. Let  $\Delta\omega_j(Y) = \omega_j(Y) - \omega_{oj}$  and  $\Delta X_j(Y) = X_j(Y) - X_{oj}$  denote, respectively, the variations of the  $j$ th-order natural frequency and the mode shape vector before and after the change, then Eq. (9) can be rewritten as

$$\begin{aligned} \lim_{\Delta K \rightarrow 0} \Delta\omega_j(Y) &= \lim_{\Delta K \rightarrow 0} \omega_j(Y) - \omega_{oj} = 0 \\ \lim_{\Delta K \rightarrow 0} \Delta X_j(Y) &= \lim_{\Delta K \rightarrow 0} X_j(Y) - X_{oj} = 0 \end{aligned} \tag{10}$$

This means that the greater damage that is made, then the larger the variation of natural frequencies and mode shape vectors. The damage defined in this case will reduce the natural frequency with respect to their original design value, and, in general, the reduction in the first mode (lowest) natural frequency is the largest.

From the view of theoretical analysis, the response in the frequency domain can be obtained by taking FFT to the time history data such that all orders of  $\omega_j(Y)$  and  $X_j(Y)$  should be determined by using their properties in the frequency domain. However, for a real situation of damage identification, only the first few eigenparameters can be available by testing. The size of the test-analysis model is typically much smaller than that of the finite element model in degrees of freedom. To provide compatibility in size between the test and analysis mode shapes, either the test mode shapes are expanded<sup>12</sup> based on the mode shapes of the structures before damage, or the system matrices are reduced.<sup>13</sup> These expanding mode techniques developed for the linear system can be generalized into identification of damage induced because of weak nonlinearity. The

reason is because the larger changes (caused by nonlinearity) appear only in the first several components in lower-order modes.

Identification of the Location of Damage

Assuming the  $j$ th-equivalent natural frequency and mode shape vector in Eq. (6a) are given by measuring and expanding techniques, Eq. (6) can be written as

$$[\Delta K_L + \Delta K_{NL}(Y)]X_j(Y) = [-K_o + \omega_j^2(Y)M_o]X_j(Y) \tag{11}$$

$j = 1, 2, \dots$

A new vector  $L$  is introduced, defined as

$$L_j(Y) = [\Delta K_L + \Delta K_{NL}(Y)]X_j(Y) = \Delta K(Y)X_j(Y) \tag{12}$$

$j = 1, 2, \dots$

where  $L_j(Y)$  is called the  $j$ th-order location vector.

Substituting Eq. (12) into Eq. (11), one obtains

$$L_j(Y) = [-K_o + \omega_j^2(Y)M_o]X_j(Y) \tag{13}$$

One can see that 1) the  $L_j(Y)$  can be determined according to Eq. (13) if the  $j$ th equivalent natural frequency and mode shape vector are available by modal testing; 2) if variation of the stiffness matrix  $\Delta K(Y) = 0$ , then  $L_j(Y) = 0$  for all  $j = 1, 2, \dots, n$ ; 3) if there exists at least a location vector, e.g.,  $j = 1$ , which satisfies  $L_j(Y) \neq 0$ , then one can determine  $\Delta K(Y) \neq 0$ , which means that the stiffness has been changed from its original form; and 4) location

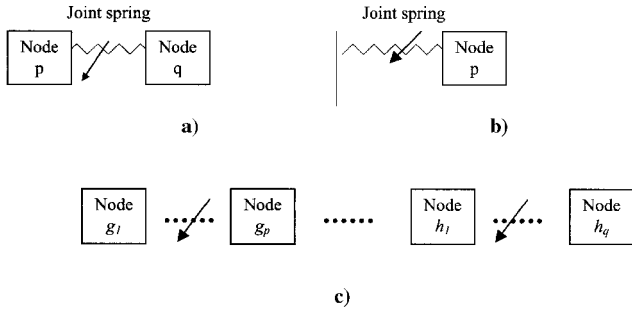


Fig. 4 Structures with damaged joints.

vectors are the functions of the amplitudes of responses only if the structure is nonlinear.

$$L_j^{(b)}(Y) = [\Delta k_{pp}(Y)] \begin{Bmatrix} X_{1j}(Y) \\ X_{2j}(Y) \\ \vdots \\ X_{nj}(Y) \end{Bmatrix}^{(b)} = \{\ell_{pj}(Y)\}^{(b)} \quad (15)$$

where  $\ell_{pj}^{(b)}(Y) = \Delta k(Y) X_{pj}^{(b)} \neq 0$ , but the rest of the components are zero in the location vector. Similar to case a, one can identify the location of damage between node  $p$  and the boundary node.

For a system with multidamaged joints, the location vector of the system can be obtained by superposing a series of location vectors of single damaged joint. For example, the assumption is made that there are two groups of the adjoining damaged joints in the structure as shown in Fig. 4c. The damaged joints are from  $g_1$  to  $g_p$  in the first group, and the damaged joints are from  $h_1$  to  $h_q$  in the second group. The location vector of the system can be written as

$$L_j^{(c)}(Y) = \begin{bmatrix} \Delta k_{g_1} & -\Delta k_{g_1} & & & \\ & \ddots & & & \\ & & \Delta k_{g_p} & & \\ & & & \text{symmetry} & \\ & & & & \Delta k_{h_1} & -\Delta k_{h_1} & & \\ & & & & \ddots & & \\ & & & & & \Delta k_{h_q} & & \end{bmatrix} \begin{Bmatrix} \vdots \\ X_{g_1} \\ \vdots \\ X_{g_p} \\ \vdots \\ X_{h_1} \\ \vdots \\ X_{h_q} \\ \vdots \end{Bmatrix} = \begin{Bmatrix} \ell_{g_1} \\ \vdots \\ \ell_{g_p} \\ \vdots \\ \ell_{h_1} \\ \vdots \\ \ell_{h_q} \end{Bmatrix}_j \quad (16)$$

The location of the damage can be found by examining the distribution of the components in the first several nonzero location vectors given. For example, the simplest case is only one damaged joint with two different connecting forms in the structures as cases a and b shown in Figs. 4a and 4b, respectively, will be considered. At the same time, letting  $\Delta k$  denote the reduction of the stiffness of this joint, then one can at least find a nonzero location vector between the first two modes. For case a, because the damaged joint is between the node  $q$  and node  $p$ , the nonzero location vector can be expressed as

$$L_j^{(a)}(Y) = \begin{pmatrix} \Delta k_{pp}(Y) & -\Delta k_{pq}(Y) \\ -\Delta k_{qp}(Y) & \Delta k_{qq}(Y) \end{pmatrix} \begin{Bmatrix} X_{1j}(Y) \\ X_{2j}(Y) \\ \vdots \\ X_{nj}(Y) \end{Bmatrix}^{(a)} = \begin{Bmatrix} \ell_{pj}(Y) \\ \ell_{qj}(Y) \end{Bmatrix}^{(a)} \quad j = 1 \text{ or } 2 \quad (14)$$

where  $\Delta k_{pp}(Y) = \Delta k_{qq}(Y) = -\Delta k_{qp} = -\Delta k_{pq} = \Delta k$ ;  $X_{ij}$  denotes the  $i$ th component of the  $j$ th mode shape vector and  $i$  is from 1 to  $n$ ;  $\ell_{ij}$ ,  $i = p, q$  denotes the  $p$ th and  $q$ th components of the  $j$ th location vector, which are corresponding to the nonzero variation value in the  $p$ th row and  $q$ th row in the variation matrix of the stiffness, respectively. On one hand, they satisfy nonzero conditions, i.e.,  $\ell_{pj}^{(a)}(Y) = \Delta k(Y)[X_{pj}(Y) - X_{qj}(Y)] = -\ell_{qj}^{(a)}(Y) \neq 0$ , but the rest of the components in the  $j$ th location vector are equal to zero. But on the other hand, their magnitudes can be determined by Eq. (13). Therefore, one can identify that the location of damage is between the node  $q$  and node  $p$  according to the distribution of nonzero components in the location vector. For case b the damaged joint is between node  $p$  and a fixed boundary so that the location vector can be expressed as

where  $\ell_i \neq \ell_{i+1} \neq 0$  for  $i = g_1, \dots, g_p$  and  $i = h_1, \dots, h_q$ , but  $\ell_i = 0$  for otherwise. From the location vector one can identify the damage locations between joints  $g_1$  to  $g_p$  and between joints  $h_1$  to  $h_q$ .

For a nonlinear damaged joint the corresponding components in the location vector are dependent on the amplitude of the responses; therefore, it can be identified by examining the location vector for different input excitations.

### Estimation of Error for LVM

LVMs are developed based on the measurement data of the equivalent eigenparameters; therefore, its estimation accuracy is dependent on the accuracy of the measurements. According to the variation form of the Eq. (13), the maximum absolute error of the location vector can be written as

$$\delta \ell_{ij}(Y) = 2 \left| \sum_{s=1}^n \omega_j(Y) m_o^{is} X_{sj}(Y) \right| \delta \omega_j + \sum_{s=1}^n \left| \omega_j^2(Y) m_o^{is} - k_o^{is} \right| \delta X_{sj} \quad i, j = 1, 2, \dots, n \quad (17)$$

where  $\delta \ell_{ij}(Y)$  denotes the maximum absolute error of the  $i$ th component of the  $j$ th location vector,  $\delta \omega_j$  denotes the maximum absolute error of the  $j$ th equivalent natural frequency, and  $\delta X_{ij}$  denotes the maximum absolute error of the  $i$ th components of the  $j$ th equivalent natural mode shape vector. The first term and the second term on the right-hand side of Eq. (17) denote the contributions to the absolute estimation error of the  $i$ th component of the  $j$ th location vector from the maximum absolute errors of the  $j$ th equivalent natural frequency and mode shape vector, respectively. Let  $\varepsilon_{ij}^{(L)}$  denote the relative estimation error of the  $i$ th component in the  $j$ th location vector,  $\varepsilon_{ij}^{(X)}$  denote the measuring relative error of the  $i$ th component in the  $j$ th equivalent normal mode shape, and  $\varepsilon_j^{(\omega)}$  denote the measuring relative error of the  $j$ th equivalent natural frequency, then, according to Eqs. (13) and (17), the relationship between them can be written as

$$\varepsilon_{ij}^{(L)}(Y) = \frac{\delta \ell_{ij}(Y)}{\ell_{ij}(Y)} = \frac{2 \sum_{s=1}^n \left| \omega_j^2(Y) m_o^{is} X_{sj}(Y) \right| \varepsilon_j^{(\omega)} + \sum_{s=1}^n \left| \omega_j^2(Y) m_o^{is} - k_o^{is} \right| \left| X_{sj}(Y) \right| \varepsilon_{mj}^{(X)}}{\left| \sum_{s=1}^n \left[ -k_o^{is} + \omega_j^2(Y) m_o^{is} \right] X_{sj}(Y) \right|} \leq \frac{\varepsilon_j^{(\omega)}}{\gamma_j(Y)} + \varepsilon_{j,\max}^{(X)}, \quad \ell_{ij}(Y) \neq 0 \quad (18)$$

where  $0 < \gamma_j(Y) = |\Delta \omega_{oj}(Y)| / \omega_{oj} < 1$  and  $\Delta \omega_{oj}(Y) = \omega_j(Y) - \omega_{oj}$  denote the relative change ratio and the absolute change value, respectively, of the  $j$ th natural frequency of the system before and after the damage and  $\omega_{oj}$  denotes the  $j$ th natural frequency of the system before the damage,  $\varepsilon_{j,\max}^{(X)} = \max\{\varepsilon_{1j}^{(X)}, \varepsilon_{2j}^{(X)}, \dots, \varepsilon_{nj}^{(X)}\}$ .

Equation (18) shows that relative estimation error of the location vector is proportional to the measuring relative errors of the natural frequencies and mode shape vectors but inverse proportional to the relative change ratio of the system before and after the damage. This means that the error of identifying the location is smaller if the degree of the damage in the structural systems is larger for the certain measuring errors of the natural frequency and mode shapes. This method can be available if  $\varepsilon_j^{(\omega)} \ll \gamma_j(Y)$  for a real situation.

### Identification of the Type and Size of the Damage

After finishing the identification of the location of the damage, it is simpler to identify the type and size of the damage. One can measure the output responses of the damaged joints in the structures for given input excitations by dynamic testing techniques. When these input/output data are obtained, it is possible to identify the size and type of the damage. In this section the identification method is developed based on such an assumption that the input data of the structures and the output data of the damaged joints can be measured.

The assumption is made that there are  $S$  damaged joints with  $2S$  unknown parameters, and the restoring force in each damaged joints can be expressed as follows:

$$f_s = k_s y_s - \alpha_s y_s^3 = k_{os} [1 - a_{1s} - a_{2s} y_s^2] y_s, \quad s = 1, 2, \dots, S \quad (19)$$

where  $y$  denotes the output of relative displacement of the  $s$ th damaged joint;  $k_{os}$  and  $k_s$  denote the linear stiffness of the  $s$ th damaged joint before and after the damage, respectively;  $\alpha_s$  denotes the nonlinear stiffness of the  $s$ th damaged joint after the damage;  $a_{1s} = (k_{os} - k_s) / k_{os}$  denotes the reduction ratio of the linear stiffness of the  $s$ th damaged joint before and after the damage and  $a_{2s} = \alpha_s / k_{os}$  denotes the ratio of the degree of nonlinearity in respect to the original linear stiffness of the  $s$ th damaged joint. At the same time, the assumption is made that system input is a harmonic excitation, then the governing equation (2) of the undamped structures can be rewritten as

$$M_o \ddot{x}(t) + K_o x(t) + \Psi \{A_1 [a_{1s} y_s(t), s = 1, \dots, S] + A_2 [a_{2s} y_s^3(t), s = 1, \dots, S]\} = B U e^{i\Omega t} \quad (20)$$

where the third and fourth terms are, respectively, equivalent to the third and fourth terms in Eq. (2);  $\Psi$  is an  $n \times S$  influence coefficient matrix of the linear term and nonlinear term of the restoring forces of the damaged joints;  $y$  is the output vector of the  $S$  nonlinear joints; and  $A_1$  and  $A_2$  are two  $S \times 1$  vectors with unknown parameters, i.e.,  $A_1 = [a_{11} y_1 \dots a_{1S} y_S]^T$  and  $A_2 = [a_{21} y_1^3 \dots a_{2S} y_S^3]^T$ .

Using FFT in Eq. (18) for the  $q$ th group of sample record data, one obtains

$$[K_o - \Omega^2(j, q) M_o] X(j, q) + \Psi \{A_1 [a_{1s} Y_s(j, q), s = 1, \dots, S] + A_2 [a_{2s} H_s(j, q), s = 1, \dots, S]\} = B U(j, q) \quad (21)$$

where

$$\begin{aligned} \Omega(j, q) &= \Omega_j^{(q)} \\ Y(j, q) &= [Y_1(j, q) \ Y_2(j, q) \ \dots \ Y_S(j, q)]^T = Y^{(q)}(\Omega_j) \\ &= \text{FFT}\{y^{(q)}(t)\} \\ X(j, q) &= X^{(q)}(\Omega_j) = \text{FFT}\{x^{(q)}(t)\} \\ H(j, q) &= H^{(q)}(\Omega_j) = \text{FFT}\{[y^3(t)]^{(q)}\} \\ U(j, q) &= U^{(q)}(\Omega_j) = \text{FFT}\{u^{(q)}(t)\} \end{aligned}$$

$J$  is the number of the discrete data of FFT, and  $Q$  is the number of groups of the sample record data. Rewriting Eq. (21) by taking away  $X(\Omega_j)$ , one obtains

$$\begin{aligned} Y(j, q) &= C [K_o - \Omega^2(j, q) M]^{-1} B U(j, q) \\ &\quad - C [K_o - \Omega^2(j, q) M]^{-1} \Psi \{A_1 [a_{1s} Y_s(j, q), s = 1, \dots, S] \\ &\quad + A_2 [a_{2s} H_s(j, q), s = 1, \dots, S]\} \end{aligned} \quad (22)$$

Substituting  $[K_o - \Omega^2(j, q) M]^{-1} = \text{adj}[K_o - \Omega^2(j, q) M_o] / \det[K_o - \Omega^2(j, q) M_o]$  into Eq. (22), the equation can be rewritten as

$$\begin{aligned} \Theta(j, q) \{A_1 [a_{1s} Y_s(j, q), s = 1, \dots, S] + A_2 [a_{2s} H_s(j, q), \\ s = 1, \dots, S]\} = D(j, q) U(j, q) - p(j, q) Y(j, q) \quad (23) \end{aligned}$$

where  $\Theta(j, q) = C E(j, q) \Psi$  is an  $S \times S$  matrix;  $E(j, q) = \text{adj}[K_o - \Omega^2(j, q) M_o]$ ;  $D(j, q) = C E(j, q) B$  is an  $S \times m$  matrix and  $p(j, q) = \det[K_o - \Omega^2(j, q) M_o]$  is a polynomial function of  $\Omega(j, q)$ . Equation (23) is an  $S \times J \times Q$  linear associated algebra equation with  $2 \times S$  unknown parameters; therefore, the equation can be solved approximately by the LSM.

### Optimum Identification

In general, most output data  $Y(j, q)$  are contaminated by noise; however, the response data in the resonance region have better signal-to-noise ratio for a real situation. Therefore, the excitation frequency  $\Omega(j)$  is chosen to equal to the natural frequencies  $\omega_o(k)$  of the original state (before the damage) of the structure, i.e.,  $\Omega^{(q)}(j_k) = \omega_o(k)$ ,  $k = 1, 2, \dots, n$ , then Eq. (23) is changed into

$$\begin{aligned} \Theta(j_k, q) \{A_1 [a_{1s} Y_s(j_k, q), s = 1, \dots, S] + A_2 [a_{2s} H_s(j_k, q), \\ s = 1, \dots, S]\} = D(j_k, q) U(j_k, q) \quad (24) \end{aligned}$$

According to the definition of vectors  $A_1$  and  $A_2$ , Eq. (24) can be rewritten as

$$\begin{aligned} \sum_{s=1}^S \theta_{ls}(j_k, q) [a_{1s} Y_s(j_k, q) + a_{2s} H_s(j_k, q)] = \sum_{i=1}^m d_{li}(j_k, q) U_i(j_k, q) \\ l = 1, 2, \dots, S, \quad q = 1, 2, \dots, Q, \quad j_n \in \{j_1, j_2, \dots, j_n\} \end{aligned} \quad (25)$$

Equation (25) can be expanded into an  $N \times 2S$  matrix as

$$\Phi A = G \quad (26)$$

where  $\Phi$  is an  $N (= n \cdot Q \cdot S) \times 2S$  coefficient matrix given by output data and it can be expressed as

$$\begin{aligned} \Phi &= [\Phi_{11} \ \Phi_{12} \ \dots \ \Phi_{1Q} \ \Phi_{21} \ \Phi_{22} \ \dots \ \Phi_{2Q} \ \dots \ \Phi_{n1} \ \Phi_{n2} \ \dots \ \Phi_{nQ}]^T \\ \Phi_{kq} &= \begin{bmatrix} \theta_{11}(j_k, q) Y_1(j_k, q) & \theta_{12}(j_k, q) Y_2(j_k, q) & \dots & \theta_{1S}(j_k, q) Y_S(j_k, q) & \theta_{11}(j_k, q) H_1(j_k, q) & \theta_{12}(j_k, q) H_2(j_k, q) & \dots & \theta_{1S}(j_k, q) H_S(j_k, q) \\ \vdots & \vdots & \dots & \vdots & \vdots & \vdots & \dots & \vdots \\ \theta_{S1}(j_k, q) Y_1(j_k, q) & \theta_{S2}(j_k, q) Y_2(j_k, q) & \dots & \theta_{SS}(j_k, q) Y_S(j_k, q) & \theta_{S1}(j_k, q) H_1(j_k, q) & \theta_{S2}(j_k, q) H_2(j_k, q) & \dots & \theta_{SS}(j_k, q) H_S(j_k, q) \end{bmatrix} \\ &\quad k = 1, 2, \dots, n, \quad q = 1, 2, \dots, Q \end{aligned}$$

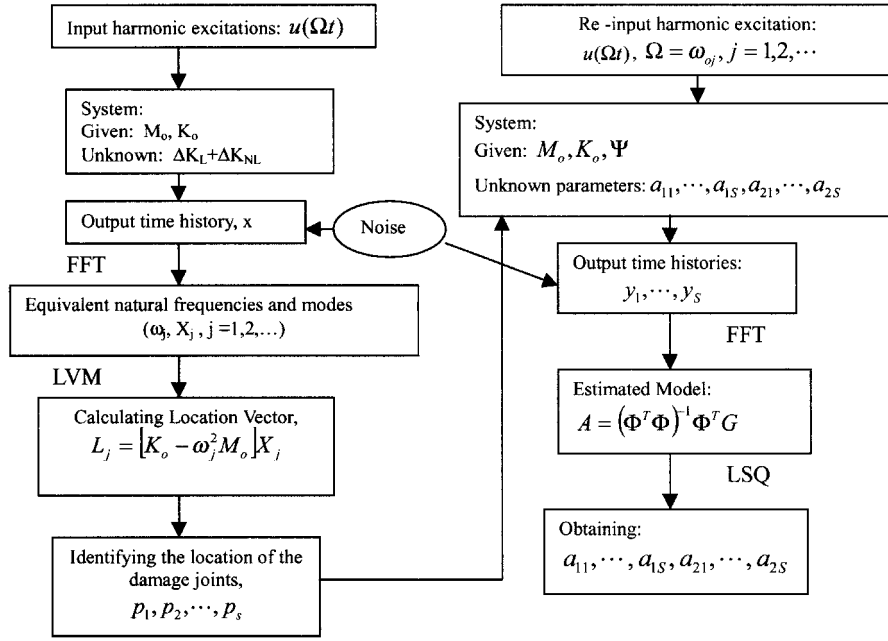


Fig. 5 Numerical simulation identification procedure.

$A$  is a vector with  $2S$  unknown parameters, i.e.,  $A = [a_{11} \ a_{12} \ \dots \ a_{1s} \ a_{21} \ a_{22} \ \dots \ a_{2s}]$  and  $G$  is a  $N \times 1$  vector given by input measuring data, i.e.,  $G = [G_{11} \ G_{12} \ \dots \ G_{1Q} \ \dots \ G_{n1} \ G_{n2} \ \dots \ G_{nQ}]^T$  and

$$G_{kq} = \left[ \sum_{i=1}^m d_{1i}(j_k, q) U_i(j_k, q) \quad \sum_{i=1}^m d_{2i}(j_k, q) U_i(j_k, q) \quad \dots \quad \sum_{i=1}^m d_{si}(j_k, q) U_i(j_k, q) \right]^T$$

By using the LSM to solve Eq. (26), the unknown vector  $A$  can be estimated, i.e.,

$$A = (\Phi^T \Phi)^{-1} \Phi^T G \quad (27)$$

To prevent the ill conditions appearing in Eq. (27), the following two conditions should be satisfied: 1)  $N > 2S$ ; and 2) all row vectors in the matrix  $\Phi$  should be linearly independent of each other, and the linear correlation row vectors should be taken away from the matrix  $\Phi$ .

### Illustrative Examples

Two examples will be discussed in this section to illustrate the identification of the location, type, and size of the damage in the structure. A five-degree-of-freedom nonlinear structure, as shown in Fig. 1, will be considered in these two examples, while assuming that 1) an input harmonic excitation  $u(t) = U \cos \Omega t$  acts on node 5 and 2) the original mass and stiffness matrices (undamaged) of the structure are, respectively,

$$M_o = m \begin{bmatrix} 1 & & & & \\ & 1 & & & \\ & & 1 & & \\ & & & 1 & \\ & & & & 1 \end{bmatrix} \quad K_o = k \begin{bmatrix} 2 & -1 & & & \\ -1 & 2 & -1 & & \\ & -1 & 2 & -1 & \\ & & -1 & 2 & -1 \\ & & & -1 & 2 \end{bmatrix} \quad (28)$$

where  $m = 1$  and  $k = 1$  are given structural parameters with dimensions.

Figure 5 shows the numerical simulation procedure in the illustration examples. In simulation procedure the output time history data are obtained by using the fourth-order Runge-Kutta method and by taking time step  $dt = 0.02$  (s). The light damp effect is

added in the simulation system to obtain the steady response under the given harmonic excitation. The response data from the frequency domain are obtained by making a FFT to the time history data in which the sample step is  $\Delta t_s = 1$  (s) and the sample number is  $N_s = 1024-2048$ . The white noise data that are generated by the white noise generator in the MATLAB® and the response contaminated by white noise are shown in Figs. 6a and 6c, respectively, in the simulation examples. The ratio of the variances of the white noise and the responses with noise is  $r \approx \sigma_{\text{white-noise}}^2 / \sigma_{\text{output}}^2 \approx 1.0498/13.7535-1.0498/8.8931 = 7-11\%$ .

**Example 1:** This identifies the location of the damaged joints. The assumptions are made that 1) joints 1 and 4 are the damaged elements and 2) their restoring forces satisfy, respectively,  $f_1(y_1) = k[(1 - a_{11})y_1 - a_{21}y_1^3]$ ,  $f_2(y_2) = k(1 - a_{12})y_2$ , where  $a_{11}$  and  $a_{12}$  denote the reduction ratios of the linear stiffness and nonlinear stiffness of the first damaged joint 1, respectively, and  $a_{12}$  denotes the reduction ratio of the second damaged joint 4 in the structure;  $y_1 = x_1$ ,  $y_2 = x_4 - x_3$ , and  $x_i$ ,  $i = 1, 2, \dots, 5$  denote the responses of the corresponding nodes in the structure.

Tables 1–4 show the information of the structural parameter, simulation input/output data of the first equivalent natural frequency and mode shape, estimation location vectors, and their estimation errors for two different cases. Figures 7a and 7b show the distribution of the components in the location vectors corresponding to two cases, respectively. One can find that joint 1 is damaged in the case 1 by  $\ell_{11} \neq 0$  in Fig. 7a and the damaged joints are joints 1 and 4 in case 2 by  $\ell_{11} \neq 0$  and  $\ell_{31} = -\ell_{41} \neq 0$  in Fig. 7b. These estimation results are coordinated with the assumption cases in Table 1.

**Example 2:** This illustrates the identification of the type and size of the damage by applying Eq. (27). The assumptions are made that 1) the damaged case is similar to the case 1 of example 1, and the unknown parameters are  $a_{11}$  and  $a_{21}$  defined in example 1 and 2) a harmonic excitation with frequency  $\Omega = \omega_{o2} = 1$  (rad/s) acts on

Table 1 Input/output information and location results in example 1: parameter values given

Case	$m$	$k$	$\omega_{o1}$	$a_{11}$	$a_{12}$	$a_{21}$	$U$	$\Omega$
a	1	1	0.5176	0.3	0	0.01	1	0.45
b	1	1	0.5176	0.2	0.25	0.01	0.5	0.4898

Table 2 Input/output information and location results in example 1: simulation of the first equivalent natural frequency and mode shape

Case	$\omega_1(Y)$	$X_{11}$	$X_{21}$	$X_{31}$	$X_{41}$	$X_{51}$
a	0.45	0.4225	0.5343	0.5384	0.4336	0.2411
b	0.4898	0.3508	0.5240	0.5728	0.4554	0.2586
	0.4962	0.3375	0.5203	0.5762	0.4625	0.2637

Table 3 Input/output information and location results in example 1: location vectors

Case	$l_{11}$	$l_{21}$	$l_{31}$	$l_{41}$	$l_{51}$
a	-0.2252	0.0006	0.0001	0.0001	0.0001
b	-0.09364	0.0013	-0.0226	0.0298	0.0003
	-0.07150	0.0011	-0.0276	0.0288	0.0001

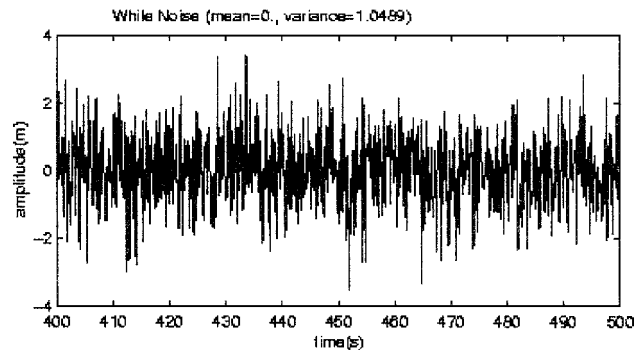


Fig. 6a White noise added into the responses in simulation experiment.

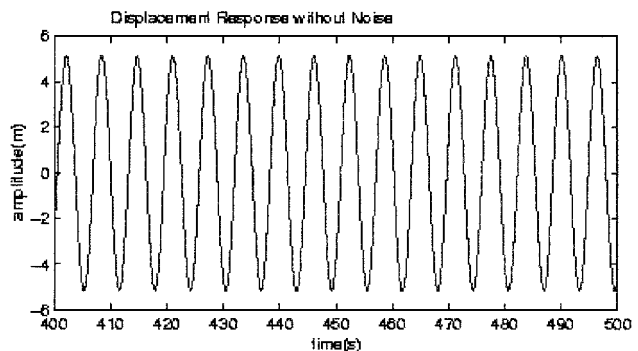


Fig. 6b Response forms before adding white noise.

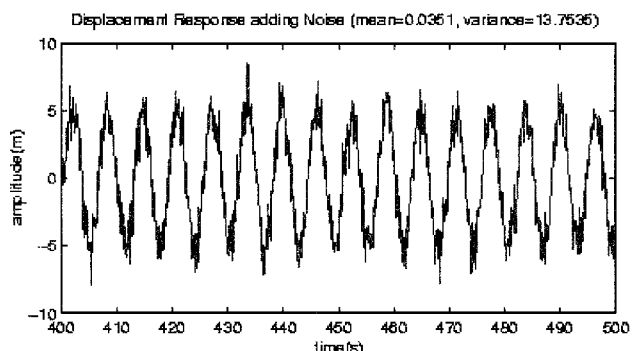


Fig. 6c Response forms after adding white noise.

Table 4 Input/output information and location results in example 1: relative errors estimation

Case	$\gamma_1, \%$	$\varepsilon_1^{(\omega)}, \%$	$\varepsilon_1^{(X)}, \%$	$\varepsilon_{11}^{(L)}, \%$	$\varepsilon_{21}^{(L)}, \%$	$\varepsilon_{31}^{(L)}, \%$	$\varepsilon_{41}^{(L)}, \%$	$\varepsilon_{51}^{(L)}, \%$
a	~13	<5	<10	<6	—	—	—	—
b	~5	<2.5	<10	<6	—	<30	<30	—
				<6	—	<30	<30	—

Table 5 Simulation of input/output data in example 2

Sample number ( $j, q$ )		Input harmonic excitation		FFT data of output response	
$j$	$q$	$\Omega(j, q), \text{rad/s}$	$U(j, q), \text{m}$	$Y(j, q)$	$H(j, q)$
1	1	1	0.5	4.05908	49.8869
1	2	1	0.75	4.66114	75.4038
1	3	1	1	5.13837	100.859

Table 6 Estimation results of unknown parameters in example 2

Estimated parameters	Exacted value	Estimated value	Error
$a_{11}$	0.0	0.0035	0.0035
$a_{21}$	0.01	0.0097	-0.0003

node 5. Under these assumptions, whereas  $M_o$  and  $K_o$  are defined in Eq. (28), the other matrices in Eq. (22) can be expressed as

$$\Psi = \begin{bmatrix} 1 \\ 0 \\ 0 \\ 0 \\ 0 \end{bmatrix}, \quad A_1 = \{a_{11}Y_1(1, q)\}, \quad A_2 = \{a_{21}H_1(1, q)\}$$
$$B = \begin{bmatrix} 0 \\ 0 \\ 0 \\ 0 \\ 1 \end{bmatrix}, \quad C = \begin{bmatrix} 1 \\ 0 \\ 0 \\ 0 \\ 0 \end{bmatrix}^T, \quad \Theta = [\theta_{11}] = [1]$$
$$D = [d_{11}] = [1]$$

(29)

Therefore, for three different groups of the sample record data with respect to different amplitudes of the input excitation, as shown in Table 5, Eq. (28) can be written as

$$\tilde{\Phi} \tilde{A} = \tilde{G}$$

(30)

where

$$\tilde{\Phi} = \begin{bmatrix} \theta_{11}Y_1(1, 1) & \theta_{11}H_1(1, 1) \\ \theta_{11}Y_1(1, 2) & \theta_{11}H_1(1, 2) \\ \theta_{11}Y_1(1, 3) & \theta_{11}H_1(1, 3) \end{bmatrix} = \begin{bmatrix} 4.05908 & 49.8869 \\ 4.66114 & 75.4038 \\ 5.13837 & 100.859 \end{bmatrix}$$
$$\tilde{G} = \begin{bmatrix} d_{11}U(1) \\ d_{11}U(2) \\ d_{11}U(3) \end{bmatrix} = \begin{bmatrix} 0.5 \\ 0.75 \\ 1. \end{bmatrix}, \quad \tilde{A} = \begin{bmatrix} \tilde{a}_{11} \\ \tilde{a}_{21} \end{bmatrix}$$

Substituting these data into Eq. (29), the unknown parameters can be estimated. The estimated results are shown in Table 6. The estimation errors are also shown in this table. One can find that the estimation results are good if the noise is absent. The case for the output contaminated by white noise (mean value = 0, and variance = 1) is investigated. The ratio between the variances of white noise and the output response is 7–11%. Table 7 shows the simulation output data contaminated with white noise and the corresponding estimation results. Figure 8 shows the comparison of the estimation results. From Table 7 and Fig. 8 one can find that the estimation results are quite satisfactory even for the case of white noise contaminated. In

Table 7 Simulated experimental input/output data contaminated with white noise (0,1)

Number	$U(1, 1) = 0.5$ $\Omega(1, 1) = 1$		$U(1, 2) = 0.75$ $\Omega(1, 2) = 1$		$U(1, 3) = 0.5$ $\Omega(1, 3) = 1$		Estimated values		Absolute errors	
	$Y(1, 1)$	$H(1, 1)$	$Y(1, 2)$	$H(1, 2)$	$Y(1, 3)$	$H(1, 3)$	$a_{11}$	$a_{21}$	$\varepsilon_{11}$	$\varepsilon_{21}$
1	4.0576	50.1036	4.6728	76.5232	5.1403	101.8654	0.0046	0.0096	$5 \times 10^{-3}$	$-4 \times 10^{-4}$
2	4.0192	48.6945	4.6315	74.5120	5.1375	101.699	0.0144	0.0091	$1 \times 10^{-2}$	$-9 \times 10^{-4}$
3	4.0607	50.2185	4.6537	75.5886	5.1870	101.667	0.0153	0.0088	$1 \times 10^{-2}$	$-1 \times 10^{-3}$
4	4.0663	50.4265	4.6592	75.8569	5.1439	102.0796	0.0044	0.0096	$4 \times 10^{-3}$	$-4 \times 10^{-4}$
5	4.0342	49.2418	4.6745	75.6276	5.1506	102.4790	0.0127	0.0091	$1 \times 10^{-2}$	$-9 \times 10^{-4}$
6	4.0117	48.4224	4.6758	76.6706	5.1220	100.7813	0.0104	0.0093	$1 \times 10^{-2}$	$-7 \times 10^{-4}$
7	4.1096	52.0546	4.6889	77.3169	5.1514	102.5267	-0.0052	0.0100	$5 \times 10^{-3}$	$4 \times 10^{-5}$
8	4.0586	50.1406	4.6601	75.9009	5.1481	102.3298	0.0069	0.0094	$7 \times 10^{-3}$	$6 \times 10^{-4}$
Mean value	4.0522	49.9128	4.6646	75.9996	5.1476	102.3035	0.0079	0.0094	$8 \times 10^{-3}$	$6 \times 10^{-4}$
Variance	$8.e-4$	1.1486	$3 \times 10^{-4}$	0.6262	$3 \times 10^{-4}$	1.074	$4 \times 10^{-5}$	$1 \times 10^{-7}$	$4 \times 10^{-5}$	$1 \times 10^{-7}$
Exacted value	4.0591	49.8869	4.6611	75.4038	5.13837	100.859	0.0	0.01	—	—

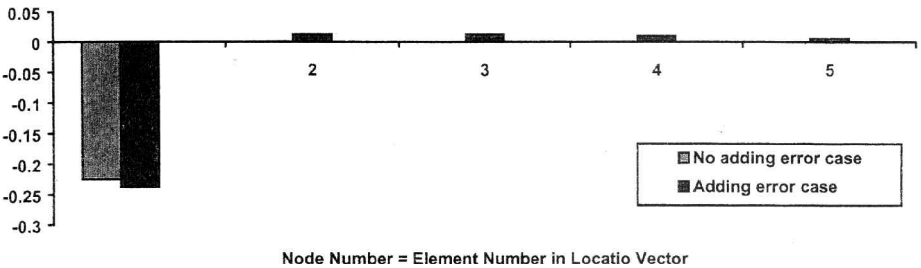


Fig. 7a Distributions of the components in the location vector for case a in example 1.

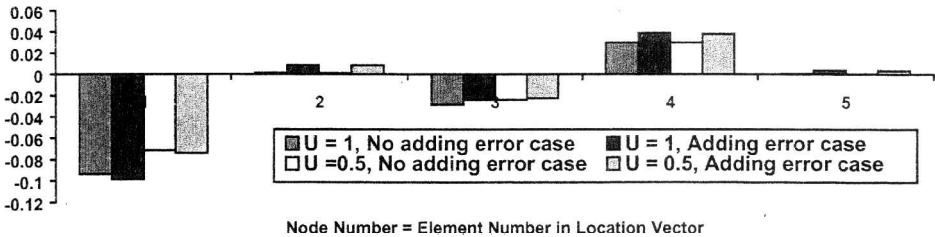


Fig. 7b Distributions of the components in the location vector for case b in example 1.

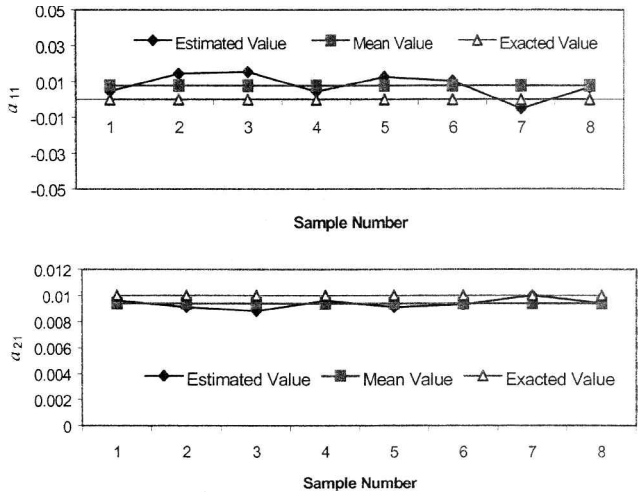


Fig. 8 Comparison of the estimation results vs a different series of the white noise in example 2.

this example for linear stiffness parameter  $a_{11}$  (exacted value = 0.0), its absolute error is less than 1%, and for nonlinear stiffness parameter  $a_{21}$  (exacted value = 0.01) its absolute error and its relative error are less than  $1.0 \times 10^{-4}$  and 1.0%, respectively.

Conclusion

A new methodology has been developed for identifying the location, type, and size of the damage in the weak nonlinear structures. It can be applied to the structures with multiple linearly or nonlinearly damaged joints and multi-input/multi-output systems. The LVM method is simple, easy, and realizable, and the estimation method for the type and size can be applicable to cases of output with white noise.

Acknowledgments

The authors are grateful that the present study was supported in part by Hong Kong Research Grant Committee Grant HKUST 12/91 and HKUST Research Infrastructure Grant RI 91/92. RC 03.

## References

- <sup>1</sup>Chen, J. C., "Structure Damage Detection for Long Suspension Bridge Under Aerodynamic Loads," *Proceedings of the Bridges into the 21st Century Hong Kong*, Hong Kong Institution of Engineers, Hong Kong, 1995, pp. 565–584.
- <sup>2</sup>Chen, J. C., and Graba, J. A., "On-Orbit Damage Assessment for Large Space Structures," *AIAA Journal*, Vol. 26, No. 9, 1988, pp. 1119–1129.
- <sup>3</sup>Berman, A., and Flannelly, W., "Theory of Incomplete Models of Dynamic Structures," *AIAA Journal*, Vol. 9, No. 8, 1971, pp. 2481–2487.
- <sup>4</sup>Zimmerman, D. C., and Simmermacher, T., "Model Correlation and System Health Monitoring Using Frequency Domain Measurements," *Proceedings of AIAA/ASME Adaptive Structures Forum*, AIAA, Washington, DC, 1995, pp. 3318–3326.
- <sup>5</sup>Ewins, D. J., *Modal Testing Theory and Practice*, Wiley, New York, 1984, pp. 82–85.
- <sup>6</sup>Brighan, E. O., *The Fast Fourier Transform and Its Applications*, Prentice-Hall, Upper Saddle River, NJ, 1989, pp. 31–70.
- <sup>7</sup>Giordano, A. A., *Least Square Estimation with Applications to Digital Signal Processing*, Wiley, New York, 1985, pp. 15–126.
- <sup>8</sup>Hairer, E., *The Numerical Solution of Differential-Algebraic Systems by Runge-Kutta Methods*, Springer-Verlag, Berlin, 1989, pp. 14–20.
- <sup>9</sup>Vidyasagar, M., *Nonlinear System Analysis*, Prentice-Hall, Upper Saddle River, NJ, 1993, pp. 88–127.
- <sup>10</sup>Szemplinska-Stupnicka, W., *The Behavior of Nonlinear Vibration System*, Kluwer Academic, Norwell, MA, 1990, pp. 114–151.
- <sup>11</sup>Cunningham, W. J., *Introduction to Nonlinear Analysis*, McGraw-Hill, New York, 1958, pp. 54–100.
- <sup>12</sup>Zimmerman, D. C., Smith, S. W., Kim, H. M., and Barkowicz, T. J., "An Experimental Study of Structural Damage Detection Using Incomplete Measurements," *Proceedings of a Collection of Technical Papers*, AIAA, Washington, DC, 1994, pp. 307–317.
- <sup>13</sup>Lim, T. W., "A Submatrix Approach to Stiffness Matrix Correction Using Modal Testing Data," *AIAA Journal*, Vol. 28, No. 6, 1990, pp. 1123–1130.

A. Berman  
Associate Editor